

Article

Benchtop Mass Spectrometry Imaging of *Eisenia Hortensis* Exposed to Statins

Kendra G. Selby [†], Claire E. Korte [†], Lauren H. Phan, Gabriel A. Bressendorff, Ashley R. Chirchirillo and Kevin R. Tucker *

Department of Chemistry, Southern Illinois University Edwardsville, Edwardsville, IL 62026, USA

* Correspondence: kevtuck@siue.edu

[†] These authors contributed equally to this work.

How To Cite: Selby, K.G.; Korte, C.E.; Phan, L.H.; et al. Benchtop Mass Spectrometry Imaging of *Eisenia Hortensis* Exposed to Statins. *Earth: Environmental Sustainability* **2025**, *1*(2), 356–365. <https://doi.org/10.53941/eesus.2025.100027>

Received: 26 September 2025

Revised: 1 December 2025

Accepted: 3 December 2025

Published: 9 December 2025

Abstract: Pharmaceuticals are contaminants of emerging concern due to their ineffective removal in wastewater treatment plants and largely unknown effects on the ecosystem. Specifically, statins are a class of blood-lipid lowering agents that are the most prescribed drug class in the United States. High concentrations of statins have been reported in water systems ranging from fresh water to wastewater. Exposure studies are frequently conducted on aquatic organisms; however, terrestrial organisms must also be assessed for accumulation of pharmaceuticals as treated wastewater is frequently used to irrigate farm fields, introducing contaminants to a greater number of species. Earthworms, specifically *Eisenia hortensis*, are frequently used as bioindicators of soil contamination. However, they have not been assessed as a bioindicator of pharmaceuticals in the environment, which this work seeks to address. Benchtop matrix-assisted laser desorption/ionization (MALDI) mass spectrometry imaging (MSI) was optimized and employed to visualize statin localization in longitudinal sections of *Eisenia hortensis* following an exposure period to atorvastatin, lovastatin, or simvastatin. All three statins were detected successfully by MSI. Lovastatin and simvastatin were ubiquitously distributed, providing evidence for both dermal absorption and ingestion of contaminated soil. Atorvastatin localized to the intestinal wall, differing from the other two analytes likely due to differences in logP values. This work suggests that *Eisenia hortensis* is a suitable bioindicator of statins in the environment.

Keywords: matrix-assisted laser desorption/ionization; linear time-of-flight; earthworm; toxicology; statins; pharmaceuticals

1. Introduction

Potable fresh water represents less than 1% of the Earth's total water supply, making it a critically limited resource. Growing concerns have emerged regarding water safety due to diverse physical, biological, and chemical pollutants that enter aquatic systems through wastewater discharge and related pathways. Current primary and secondary wastewater treatment practices effectively remove physical and biological contaminants such as sediments, organic matter, and pathogens; however, they do little to eliminate chemical contaminants like heavy metals, pesticides, and pharmaceuticals [1]. These are mainly targeted at the tertiary level of treatment (e.g., UV disinfection, activated carbon), where removal is improved but remains incomplete [2]. To further exacerbate the issue, many wastewater treatment plants terminate the treatment process at the secondary level, particularly in rural areas due to prohibitive costs, leaving chemical contaminants largely unaddressed. In addition to pharmaceuticals, other micropollutants such as antibiotics, hormones, and personal care products are also present



Copyright: © 2025 by the authors. This is an open access article under the terms and conditions of the Creative Commons Attribution (CC BY) license (<https://creativecommons.org/licenses/by/4.0/>).

Publisher's Note: Scilight stays neutral with regard to jurisdictional claims in published maps and institutional affiliations.

at trace levels in treated effluent, often persisting long enough to enter both aquatic and terrestrial systems. This cocktail of contaminants highlights the challenge of addressing cumulative exposure risks in environments that rely heavily on reclaimed water for irrigation or discharge into natural waterways.

Pharmaceuticals are a notable class of environmental contaminants of emerging concern due to their biological activity at low concentrations [3] and incomplete removal in wastewater treatment plants [2], leading to measurable concentrations of pharmaceuticals found in wastewater effluent [4]. These pharmaceuticals can have toxic effects on non-target organisms, especially in aquatic systems [5]. Although aquatic organisms have traditionally been emphasized in ecotoxicology studies, the terrestrial component is increasingly important. The reuse of treated wastewater for agricultural irrigation exposes soil invertebrates and plants directly to residual pharmaceuticals, creating pathways for uptake into terrestrial food webs. Soil organisms are therefore not only at risk themselves but may also act as vectors, transferring contaminants to higher trophic levels such as birds and small mammals. It is critical to study the previously unknown effects of pharmaceutical contaminants on various organisms to assess greater harm to the ecosystem.

Specifically, statins are a class of pharmaceuticals that work to decrease low density lipoprotein (LDL), commonly referred to as “bad cholesterol” [6]. They have remained the most prescribed class of drugs in the United States since the 1990s [7]. As such, statins have been detected in the environment at the low ppb range [8–10]. Given their widespread prescription rate, statins represent an important pharmaceutical class for environmental toxicology.

Earthworms (*Eisenia*) are established bioindicators in soil toxicology, with *E. fetida* commonly used for organic contaminants and *E. hortensis* for heavy metals [11–18]. However, little is known about the suitability of *E. hortensis* for pharmaceutical exposure studies, representing a gap this work seeks to address. It is important to determine if *E. hortensis* can be a potential bioindicator for pharmaceutical exposures because treated wastewater that contains pharmaceuticals is frequently used for crop irrigation [19]. Moreover, *E. hortensis* have been shown to dwell in agricultural soils [20], whereas *E. fetida* are more likely to thrive in compost [12], further highlighting their potential for studying environmental exposure. As such, agricultural irrigation conditions can be modeled in a laboratory exposure with garden soil to assess the uptake of pharmaceuticals into earthworm tissue. Earthworms are a critical link in terrestrial food webs, thus, bioaccumulation of pharmaceuticals in their tissues has ecological implications that extend beyond soil health, such as the potential transfer of these compounds into higher trophic levels. Establishing *E. hortensis* as a pharmaceutical bioindicator therefore serves both practical monitoring purposes and broader ecological relevance, strengthening its utility in environmental risk assessments.

Mass spectrometry imaging (MSI), particularly matrix-assisted laser desorption/ionization (MALDI) MSI, integrates the sensitivity of conventional MS with two-dimensional spatial resolution. Separation based MS is well-established for environmental analysis, offering identification and quantitation of contaminants at low concentrations using targeted and untargeted methods, however, spatial distribution is lost in the sample preparation as tissues are homogenized and analytes extracted prior to analysis. In contrast, MSI preserves tissue architecture, enabling visualization of both endogenous and exogenous compounds including active pharmaceutical ingredients (APIs) and their metabolites. Applications have expanded from biomedical contexts, ranging from mapping neuropeptides [21] to emerging environmental studies [22,23]. For context, MALDI MSI works by coating a thin (approximately 10 µm) [24] slice of tissue in a layer of an organic acid or base (i.e., matrix) for cocrystallization with the sample containing analytes of interest. A laser is then used to ablate the solid mixture, causing the matrix and analytes to desorb from the surface and ionize allowing MS to proceed. Imaging also enables analysis of compounds found in high local concentration but low global concentration within the tissue without risking inherent sample loss and increasing sample preparation complexity induced from homogenization. MSI has been previously demonstrated to identify the specific tissue or region where contaminants are accumulating, so it can then be isolated and analyzed [22]. MSI can detect not only the API, but also the biological metabolites produced by the living species. Furthermore, the specific tissue and locations within the tissues can provide critical information about the pathways of uptake of an API, the effect(s) on the organism, and possible degradation mechanisms [23]. In summary, MSI can enable rapid discoveries that are otherwise forfeited due to homogenization of samples prior to analysis.

Detecting an array of contaminants and metabolites directly from the tissues requires high mass resolution and sensitivity. Reflectron time-of-flight (reTOF) and hybrid analyzers (e.g., quadrupole TOF) are typically employed as a result when non-targeted analysis is sought [23]. While these instruments are present in well-funded research labs and core facilities, funding for environmental science research is typically less abundant. As a result, the optimization and use of benchtop linear TOF instruments is more accessible in environmental sciences and works well for targeted analysis but comes at the expense of both mass resolution and spatial resolution. Due to reduced sensitivity, the spatial resolution of linear instruments is typically lower (>50 µm) to achieve detection. Imaging experiments require optimization of sample preparation and instrumental parameters to achieve detection

of low-concentration analytes of different classes within the same tissue and increase spatial resolution. This optimization is particularly critical in the case of linear TOF instruments with poorer figures of merit.

Eisenia hortensis has been established as a biomonitor for environmental contamination; however, more research is necessary to expand this role beyond heavy metals. The goal of this work is to develop an optimized method to complement previous work imaging lipid related species [18] to now image the APIs in *Eisenia hortensis* tissue after exposure to environmentally relevant concentrations of statins using MSI. Specifically, atorvastatin, lovastatin, and simvastatin will be investigated due to their high prescription rate [7] and targeting lipophilic compounds that were shown previously [18]. Localization will be determined utilizing a benchtop linear MALDI-TOF instrument to enhance accessibility within the environmental science research sector.

2. Materials and Methods

2.1. Standards and Reagents

Pharmaceutical standards of atorvastatin (ATO; CRM; P/N: PHR1422), lovastatin (LOV; >98%; P/N: L0214), and simvastatin (SIM; 98%; P/N: 458840250) were purchased from Sigma Aldrich (St. Louis, MO, USA), Tokyo Chemical Industry (Tokyo, Japan), and Thermo Fisher Scientific (Waltham, MA, USA), respectively. α -cyano-4-hydroxycinnamic acid (CHCA; 97%; P/N: 145505) was purchased from Sigma Aldrich (St. Louis, MO, USA). HPLC-grade methanol (P/N: AA22909K2) was purchased from Thermo Fisher Scientific (Waltham, MA, USA), and biotechnology grade trifluoroacetic acid (TFA; P/N: 89399-844) was purchased from VWR (Radnor, PA, USA). ACS-grade ammonium sulfate (P/N: 423400250) was purchased from Thermo Fisher Scientific (Waltham, MA, USA). Water refers to Type 1 water unless otherwise specified. Soil was obtained as garden soil from a local hardware store.

2.2. Earthworm Care and Exposure

Eisenia hortensis (Speedy Worm, Alexandria, MN, USA) were cared for and exposed to statins dissolved in water as described previously [18]. The worms were exposed to 100-fold of their environmentally reported concentrations, as shown in Table 1. This elevated concentration was selected deliberately to address the sensitivity limitations of benchtop linear TOF instruments. At environmentally realistic levels (low ppb range), statins fall below the instrument's detection threshold, particularly when distributed heterogeneously in tissue. By applying a 100× enrichment, exposures remained within a non-lethal range for the worms while generating signals strong enough to validate method performance and visualize tissue localization. This scaling approach is commonly used in environmental toxicology to establish proof-of-concept imaging workflows before moving toward more realistic concentrations with higher sensitivity platforms.

Table 1. Relevant concentrations of atorvastatin (ATO), lovastatin (LOV), and simvastatin (SIM).

Compound	Environmental Concentration (ppb)	Exposure Concentration (ppb)
ATO [8]	0.2	20
LOV [9]	0.1	10
SIM [10]	1.5	150

Spiked soils were prepared by homogenizing garden soil with aqueous pharmaceutical standards and allowing the mixture to equilibrate to ensure even contaminant distribution. Moisture content was maintained between 20–30% with daily monitoring [18]. Each treatment consisted of 20 replicate worms housed in ventilated containers, alongside controls maintained in untreated soil. This approach was designed to mimic realistic agricultural irrigation scenarios while ensuring exposures were controlled and reproducible.

2.3. Euthanasia and Cryosectioning

Following a two-week exposure to one of the statins (ATO, LOV, or SIM) at 100-fold of the environmental concentration, earthworms were euthanized by flash freezing. Specifically, earthworms were individually collected, rinsed with water, and arranged in a metal bottle cap (to enable mounting on a circular chuck) secured with aluminum foil and flash frozen in liquid nitrogen. Prepared earthworms were stored at −40 °C until sectioning. Cryosectioning was performed on a Leica CM 1850 cryostat (Leica, Deer Park, IL, USA) at −20 °C. Water was placed onto a frozen chuck, where it froze into a dome shape. The dome of water was shaved down to a flat surface with the cryostat before placing the coiled, frozen worm onto the surface of the ice with no overlap of tissue as shown in Figure 1. More water was added and allowed to freeze, creating a dome of ice on and around the frozen worm tissue. 100 μ m

sections of ice and worm tissue were shaved off until the gut of the worm was exposed, at which point 20 μm sections of worm tissue were obtained. Two sections from each worm were thaw-mounted onto individual indium tin oxide-coated glass slides (Shimadzu Scientific Instruments, Columbia, MD, USA). This coiling and embedding method minimized tissue folding and tearing, ensuring high-quality sections suitable for MSI. The 20 μm thickness was chosen as a compromise between structural integrity and spatial resolution of imaging.

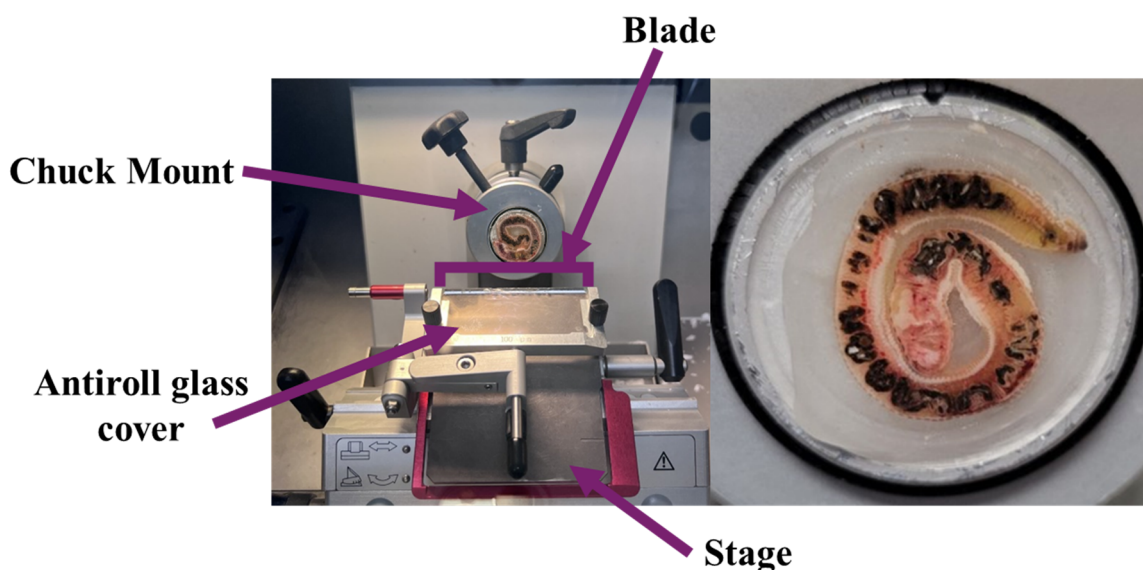


Figure 1. Cryostat Workstation and Worm During Cryosectioning. Shown on the left side of the image is the interior of the cryostat during use, with several key components labeled. The right side of the image shows an ice-covered chuck with a mounted earthworm that has been transversely sectioned.

2.4. Matrix Application and Salt Wash

Slides were dried in a vacuum desiccator and washed with salt prior to matrix deposition to enhance statin ionization. The previous method [18] made use of a 5 s wash in 50 mM ammonium sulfate to enhance the lipid signal; in this study, the salt concentration was optimized to 5 mM for increased statin ionization. Each slide was individually submerged into the 5 mM ammonium sulfate solution for 5 s and allowed to dry prior to matrix application.

A handheld artist airbrush sprayer (Paasche VL 0123, Kenosha, WI, USA) powered by an air compressor (Master 17 Airbrush TC-320, Las Vegas, NV, USA) was used to deposit 50 mL of 10 mg/mL CHCA in methanol with 0.1% (v/v) TFA onto the slide. To ensure consistency of application, the slide was placed the same distance away from the sprayer each time and sprayed at a consistent angle and pressure for the same number of passes. The airbrush method was selected over sublimation and automated sprayers due to its cost-effectiveness and adaptability in smaller research settings. Although sublimation provides finer crystal formation and uniform coatings, the airbrush allowed rapid adjustments of deposition thickness and solvent composition during optimization of statin signal.

Matrix was removed from a corner of the imaging window that was absent of tissue using methanol and a cotton-tipped applicator. To this location, 0.5 μL of CHCA and 0.5 μL of TOFMix (LaserBio Labs; Valbonne, France) were spotted according to the dried droplet method for mass calibration. In addition to the peptides contained in TOFMix, matrix peaks were utilized to ensure low mass calibration. This calibration ensured accurate mass assignment for the statin parent compounds, compensating for the reduced resolving power of the benchtop linear TOF instrument. A slide fully prepared for data acquisition can be seen in Figure 2.

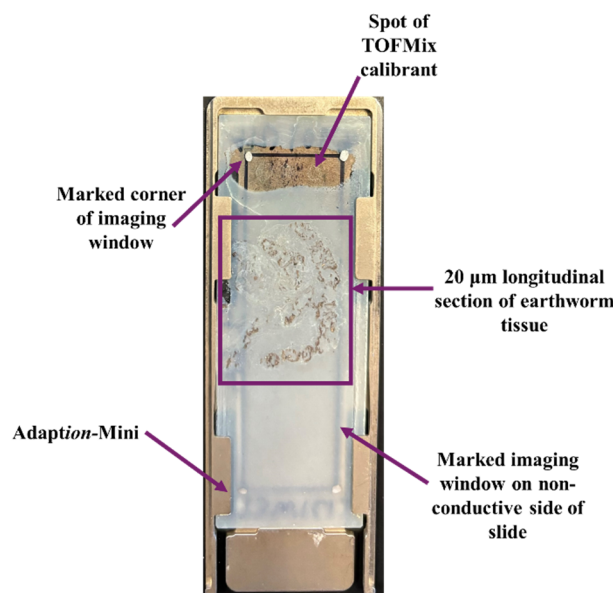


Figure 2. A Slide Fully Prepared for MALDI MSI Analysis on a Shimadzu MALDI-8020. This sample preparation workflow described here outlines several steps that are unique to analysis on this instrument, including tracing the imaging window, marking the corners of the imaging window, and the use of the Adaption-Mini.

2.5. MALDI MSI Analysis

The instrument used for this analysis was the Shimadzu MALDI-8020 (Shimadzu Scientific Instruments, Columbia, MD, USA), a benchtop instrument with a frequency-tripled 200 Hz Nd:YAG solid state laser (355 nm) and a positive linear TOF mass analyzer (<1 m). Data acquisition and mass spectral processing were performed using MALDI Solutions Data Acquisition (Shimadzu Scientific Instruments, Columbia, MD, USA); image generation and processing were accomplished using IonView (Shimadzu Scientific Instruments, Columbia, MD, USA). Laser power was set to an arbitrary value of 90, on a scale from 0 to 180. Data was acquired with a mass range from 300–1100 m/z , and pulsed extract of 1500 Da. Twenty mass spectra were obtained at each pixel with a spatial resolution of $100 \times 100 \mu\text{m}$ and a repetition rate of 100 Hz.

Although hybrid TOF or Orbitrap instruments offer superior mass resolution and sensitivity, the choice of the MALDI-8020 emphasizes accessibility and affordability in laboratories with limited resources. The tradeoff was a decrease in spatial resolution and sensitivity, necessitating optimization of both laser power and matrix deposition to reliably detect low-abundance analytes. The acquisition settings were selected after iterative trials that balanced throughput and data quality.

3. Results

Matrix optimization had previously been performed to enhance cholesterol signal as a representative lipid analyte [18]. The present work has focused on detection of the statin parent compounds at the expense of lipid signal, as endogenous lipids are far more abundant than the statin contaminants. Alternative MALDI matrices (2,5-dihydroxybenzoic acid and sinapinic acid) were also tested in preliminary trials; however, CHCA provided superior ionization efficiency and reproducibility for statins, and thus was selected for all subsequent experiments. However, in this study, a 5 s salt wash in 5 mM ammonium sulfate was found to sufficiently reduce the lipid signal to enable statin detection, an alteration from the previous 50 mM wash. As observed in Figure 3, the 5 mM wash was able to remove most of the signal from cholesterol. Longer rinses were characterized by greater removal of polar compounds, including statins, thus more intense signal from cholesterol and other lipids (see previous method [18]).

MALDI-MSI images of earthworms exposed to 100-fold of the environmentally relevant concentrations of atorvastatin, lovastatin, and simvastatin are shown in Figure 4. Control worms are shown in Figure S1 for comparison. As demonstrated in Table 2, the sodiated adduct ($[M+Na]^+$) was observed in situ for all three pharmaceuticals, with ATO and LOV also forming the protonated ($[M+H]^+$) and potassiated adducts ($[M+K]^+$), respectively. ATO signal was primarily observed in the gut region of the earthworm section, whereas LOV was more localized to the dermis of the earthworm on the exterior of the section. The SIM signal yielded a more uniform distribution across the section, with a slight localization in the head region of the earthworm. In addition

to tissue distribution, adduct formation provided indirect insight into the chemical microenvironments of different regions. The consistent appearance of $[M+Na]^+$ for all three statins suggests that sodium ions present in worm tissue strongly influence ionization pathways. Atorvastatin's ability to also form $[M+H]^+$ may reflect localized proton-rich environments in the gut, while lovastatin's $[M+K]^+$ adduct indicates interaction with potassium-dense dermal regions. These distinctions highlight how MSI can capture subtle biochemical differences across tissues that may affect pharmaceutical uptake and retention.

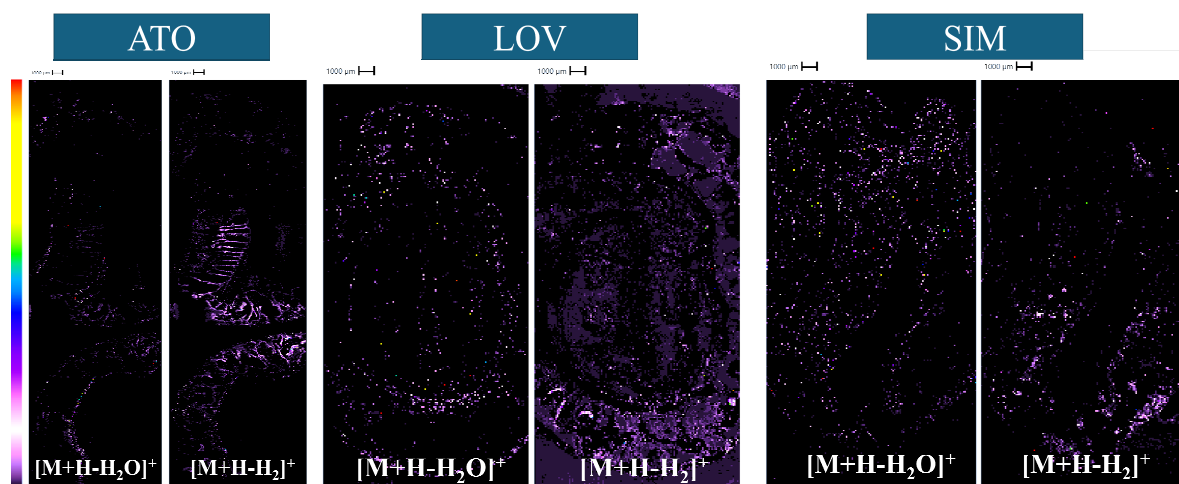


Figure 3. Distribution of Cholesterol in Earthworms Exposed to Statins. Earthworms were exposed to either atorvastatin (ATO), lovastatin (LOV), or simvastatin (SIM). 50 mL of 10 mg/mL CHCA was applied via artist airbrush sprayer. The images shown here represent the signal generated by an adduct of the cholesterol normalized to the TIC. The appropriate adduct is indicated on the lower border of each image.

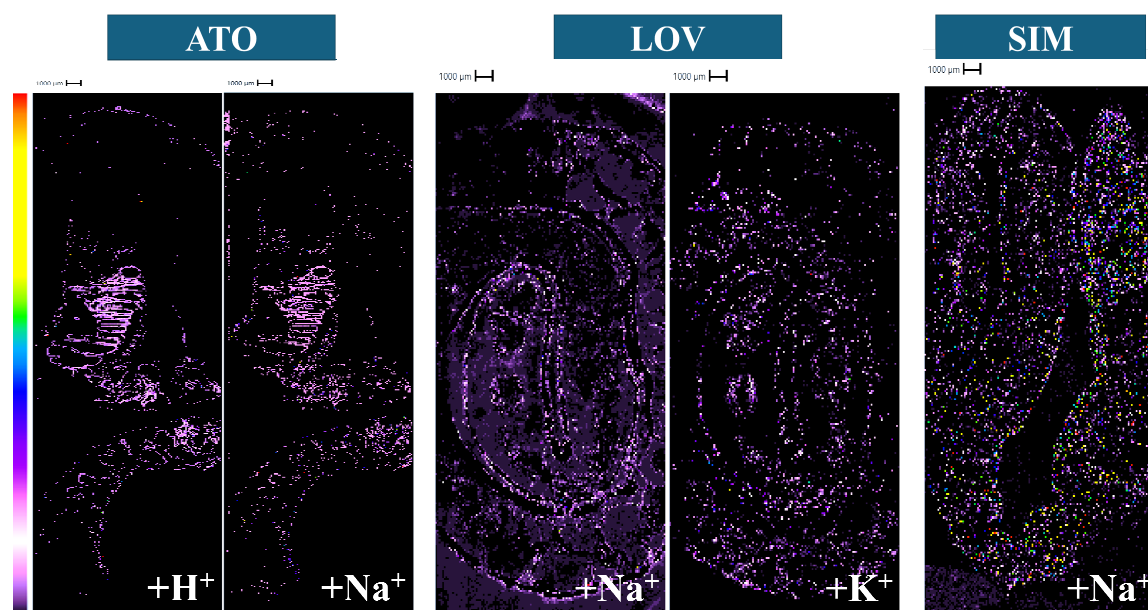


Figure 4. Distribution of Statins in Exposed Earthworms. Earthworms were exposed to either atorvastatin (ATO), lovastatin (LOV), or simvastatin (SIM). The images shown here represent the signal generated by an adduct of the statin parent compound normalized to the TIC. The appropriate adduct is indicated in the lower right corner of each image.

Table 2. Observed and chemical properties of atorvastatin, lovastatin, and simvastatin (logP values obtained from DrugBank).

	Nominal Mass	Observed $[M+H]^+$	Observed $[M+Na]^+$	Observed $[M+K]^+$	logP
ATO	558	559	581	597	6.36
LOV	404	405	427	443	4.08
SIM	418	419	441	457	4.68

While quantitation from these images is not feasible, the images still inform future experiments where parts of the worm anatomy could be dissected for quantitation. Comparison with an uptake study in mammals shows a similar trend: more lipophilic compounds, such as atorvastatin (logP 6.36), localize preferentially to lipid-rich membranes, while less lipophilic analogues distribute more broadly [25]. This correlation between logP values and observed distributions reinforces the predictive value of physicochemical properties in environmental bioaccumulation research.

Importantly, the visualization of distinct statin localization at sub-millimeter resolution demonstrates that even benchtop MSI platforms can generate biologically meaningful data. Although the worms were exposed to elevated concentrations to overcome sensitivity limits, the observed tissue-level patterns provide a foundation for future quantitative studies at environmentally realistic doses.

4. Discussion

In the previous method [18], matrix images were initially assessed to determine whether a particular matrix offered uniform coverage of the tissue in the imaging region. This step was not performed here given that CHCA has already been established as the preferred matrix for cocrystallization with analytes in earthworm tissue.

Cholesterol was initially examined because it is common throughout biological tissue and has well established and notable MS signals at 369 m/z ($[M+H-H_2O]^+$) and 385 m/z ($[M+H-H_2]^+$) [26]. In the worm exposed to ATO, the two ions exhibit different spatial distributions, with the dehydrated ion localizing to the dermal region of the earthworm, whereas the other ion is more prevalent in the interior of the body (Figure 4). The dehydrated form may appear localized to the dermis as an artifact of flash freezing. The same pattern is observed for the worms exposed to LOV and SIM, but it is more difficult to definitively conclude due to the sparse apparent distribution. In all cases, cholesterol was poorly ionized following a 5 mM salt wash compared with the previous 50 mM salt wash.

MSI enabled visualization of statin localization, which served as evidence for the uptake and accumulation of statins by *E. hortensis*. Even with low spatial resolution, differences in accumulation between large organs are clearly visible within the earthworm tissue. Higher spatial resolution instruments would be necessary to resolve accumulation differences between finer tissue structures. The distribution of the statins herein provides insight into possible routes of accumulation of the three compounds. LOV and SIM differ only by a single methyl group, likely leading to their similar distribution throughout the body of the worm. SIM is more ubiquitously distributed than LOV in the images, likely due to the high exposure concentration of SIM, which is 15-fold higher than LOV. It is noted that LOV could show a more ubiquitous distribution at higher exposure concentration. Overall, the spatial patterns of these two molecules suggest both ingestion of contaminated soil as well as absorption of contaminants through the dermis.

ATO has a unique spatial distribution, with localization observed in the intestinal region of the earthworm. This drug has a higher logP value, listed in Table 2, than the other two statins, making it more attracted to the hydrophobic lipid bilayer present in the intestinal wall. This intestinal localization suggests that ingestion of contaminated soil is the predominant route of accumulation. This observation is consistent with prior studies, where lipophilic pharmaceuticals preferentially accumulated in lipid-rich tissues such as liver or membranes, whereas less lipophilic compounds distributed more broadly. These parallels strengthen confidence that logP is a predictive parameter for uptake pathways. Such information is critical to determine the mechanism of degradation or metabolism of the APIs, which is important for developing vermiremediation applications. One study found that atorvastatin was significantly less toxic to *E. fetida* than simvastatin and lovastatin [11], providing insight into possible tissue-specific effects of the statins on various earthworm species depending on the localization of the different drugs. Some studies have shown the activation of metabolic pathways in *C. elegans* exposed to statins [27], but no studies have shown earthworm-specific metabolism and toxic effects, especially not with spatial information. Further metabolic and toxicology studies should be completed using *E. hortensis* as a model organism following exposure to statins to elucidate tissue-specific effects and/or degradation products. For example, if earthworms sequester statins primarily in intestinal tissues, as shown with atorvastatin, enzymatic or microbial communities within the gut could be targeted for studying biotransformation products in future work. This opens a path to investigate whether earthworms can not only serve as sentinels but possibly play an active role in contaminant remediation, or elucidate specific toxic effects.

Ultimately, the present data suggests that a wash with 5 mM ammonium sulfate prior to matrix deposition is sufficient for statin ionization but insufficient for lipid ionization; on the other hand, the previously described 50 mM wash prevented statin ionization while providing lipid ionization. It is worth noting that the earthworm images were obtained after exposure to 100-fold of the concentration found in the environment. This concentrated exposure was necessary to reach the limits of detection and demonstrate the potential of *E. hortensis* as a model species.

While this proof-of-concept approach used elevated doses, future studies could combine benchtop MSI with high-sensitivity quantitative assays (LC–MS/MS) to confirm uptake at environmentally relevant levels. Additionally, coupling imaging data with behavioral or physiological endpoints in *E. hortensis* could provide a holistic understanding of pharmaceutical impact. Beyond statins, extending this framework to other commonly prescribed drug classes (e.g., antidepressants, antibiotics) will broaden the ecological relevance of earthworm models.

From a methodological standpoint, this study demonstrates the practicality of benchtop MALDI MSI in environmental sciences. While resolution and sensitivity are lower compared to other platforms, the accessibility of benchtop instruments enables wider adoption. This expansion of MSI tools is critical in a field where funding constraints often limit the use of cutting-edge instrumentation. Thus, the ability to visualize contaminant localization with affordable platforms has significant implications for scaling environmental monitoring across academic and regulatory labs.

5. Conclusions

This study demonstrates that benchtop MALDI MSI can be successfully applied to visualize statins in *E. hortensis* tissues, revealing distinct uptake pathways linked to compound lipophilicity. Statins were localized to distinct tissue regions in *E. hortensis*, suggesting uptake via both dermal absorption and ingestion. The visualization of statins in *E. hortensis* demonstrates their utility as a biomarker for pharmaceutical contamination, with the opportunity for future analyses to delve into degradation and toxicity mechanisms. Beyond methodological proof-of-concept, this work illustrates the value of accessible instrumentation in environmental toxicology. By adapting workflows for benchtop MSI, laboratories with limited resources can still generate biologically meaningful spatial data, enabling wider participation in contaminant monitoring. These findings highlight the potential of benchtop MSI platforms for environmental applications and underscore the need for further method refinement to enable simultaneous lipid–pharmaceutical imaging. If statins and lipids are to be imaged in the same sample, salt wash concentration and composition must be further studied. Looking ahead, coupling imaging with physiological/behavioral analyses, quantitative analyses, metabolite tracking, and cross-species comparisons will extend the utility of earthworm models and provide a fuller picture of pharmaceutical effect and fate in terrestrial ecosystems.

Supplementary Materials

The additional data and information can be downloaded at: <https://media.sciltp.com/articles/others/2512081437168305/EESUS-25090118-Supplementary-Materials.pdf>. Figure S1: Distribution of Statins in Control Earthworms. Earthworms were exposed to equal volumes of water as opposed to statin dosing solution. The images shown here represent the signal generated by an adduct of the statin parent compound normalized to the TIC. The appropriate adduct is indicated in the lower right corner of each image.

Author Contributions

K.G.S.: Conceptualization; Data Curation; Formal Analysis; Funding Acquisition; Investigation; Methodology; Visualization; Writing—review & editing. C.E.K.: Data Curation; Formal Analysis; Investigation; Visualization; Writing—original draft; Writing—review & editing. L.H.P.: Investigation. G.A.B.: Investigation. A.R.C.: Investigation. K.R.T.: Conceptualization; Funding Acquisition; Project Administration; Resources; Supervision; Writing—review & editing. All authors have read and agreed to the published version of the manuscript.

Funding

This work was supported by the National Science Foundation through award # DUE 2130471. Any opinions, findings, and conclusions or recommendations expressed in this material are those of the author(s) and do not necessarily reflect the views of the National Science Foundation. Additionally, this work was supported by the Research Grants for Graduate Students and Undergraduate Research and Creative Activities programs internally at SIUE.

Institutional Review Board Statement

Not applicable.

Informed Consent Statement

Not applicable.

Data Availability Statement

Raw data can be provided upon request to the corresponding author.

Conflicts of Interest

The authors declare no conflict of interest.

Use of AI and AI-Assisted Technologies

No AI tools were utilized for this paper.

References

1. Matesun, J.; Petrik, L.; Musvoto, E.; et al. Limitations of Wastewater Treatment Plants in Removing Trace Anthropogenic Biomarkers and Future Directions: A Review. *Ecotoxicol. Environ. Saf.* **2024**, *281*, 116610. <https://doi.org/10.1016/j.ecoenv.2024.116610>.
2. Belete, B.; Desye, B.; Ambelu, A.; et al. Micropollutant Removal Efficiency of Advanced Wastewater Treatment Plants: A Systematic Review. *Env. Health Insights* **2023**, *17*, 11786302231195158. <https://doi.org/10.1177/11786302231195158>.
3. Daughton, C.G.; Ternes, T.A. Pharmaceuticals and Personal Care Products in the Environment: Agents of Subtle Change? *Env. Health Perspect.* **1999**, *107*, 907–938. <https://doi.org/10.1289/ehp.99107s6907>.
4. Nikolaou, A.; Meric, S.; Fatta, D. Occurrence Patterns of Pharmaceuticals in Water and Wastewater Environments. *Anal. Bioanal. Chem.* **2007**, *387*, 1225–1234. <https://doi.org/10.1007/s00216-006-1035-8>.
5. Ben Chabchoubi, I.; Lam, S.S.; Pane, S.E.; et al. Hazard and Health Risk Assessment of Exposure to Pharmaceutical Active Compounds via Toxicological Evaluation by Zebrafish. *Environ. Pollut.* **2023**, *324*, 120698. <https://doi.org/10.1016/j.envpol.2022.120698>.
6. Maron, D.J.; Fazio, S.; Linton, M.F. Current Perspectives on Statins. *Circulation* **2000**, *101*, 207–213. <https://doi.org/10.1161/01.CIR.101.2.207>.
7. Kantor, E.D.; Rehm, C.D.; Haas, J.S.; et al. Trends in Prescription Drug Use Among Adults in the United States From 1999–2012. *JAMA* **2015**, *314*, 1818–1830. <https://doi.org/10.1001/jama.2015.13766>.
8. Ottmar, K.J.; Colosi, L.M.; Smith, J.A. Fate and Transport of Atorvastatin and Simvastatin Drugs during Conventional Wastewater Treatment. *Chemosphere* **2012**, *88*, 1184–1189. <https://doi.org/10.1016/j.chemosphere.2012.03.066>.
9. Conley, J.M.; Symes, S.J.; Schorr, M.S.; et al. Spatial and Temporal Analysis of Pharmaceutical Concentrations in the Upper Tennessee River Basin. *Chemosphere* **2008**, *73*, 1178–1187. <https://doi.org/10.1016/j.chemosphere.2008.07.062>.
10. Barros, S.; Coimbra, A.M.; Alves, N.; et al. Chronic Exposure to Environmentally Relevant Levels of Simvastatin Disrupts Zebrafish Brain Gene Signaling Involved in Energy Metabolism. *J. Toxicol. Environ. Health Part A* **2020**, *83*, 113–125. <https://doi.org/10.1080/15287394.2020.1733722>.
11. Pino, M.R.; Val, J.; Mainar, A.M.; et al. Acute Toxicological Effects on the Earthworm *Eisenia Fetida* of 18 Common Pharmaceuticals in Artificial Soil. *Sci. Total Environ.* **2015**, *518–519*, 225–237. <https://doi.org/10.1016/j.scitotenv.2015.02.080>.
12. IndraKumar Singh, S.; Singh, W.R.; Bhat, S.A.; et al. Vermiremediation of Allopathic Pharmaceutical Industry Sludge Amended with Cattle Dung Employing *Eisenia Fetida*. *Env. Res.* **2022**, *214*, 113766. <https://doi.org/10.1016/j.envres.2022.113766>.
13. Singh, D.; Suthar, S. Vermicomposting of Herbal Pharmaceutical Industry Waste: Earthworm Growth, Plant-Available Nutrient and Microbial Quality of End Materials. *Bioresour. Technol.* **2012**, *112*, 179–185. <https://doi.org/10.1016/j.biortech.2012.02.101>.
14. McKelvie, J.R.; Wolfe, D.M.; Celejewski, M.A.; et al. Metabolic Responses of *Eisenia fetida* after Sub-Lethal Exposure to Organic Contaminants with Different Toxic Modes of Action. *Environ. Pollut.* **2011**, *159*, 3620–3626. <https://doi.org/10.1016/j.envpol.2011.08.002>.
15. Vergara-Luis, I.; Rutkowski, C.F.; Urionabarrenetxea, E.; et al. Antimicrobials in *Eisenia Fetida* Earthworms: A Comprehensive Study from Method Development to the Assessment of Uptake and Degradation. *Sci. Total Environ.* **2024**, *922*, 171214. <https://doi.org/10.1016/j.scitotenv.2024.171214>.
16. Carter, L.J.; Ryan, J.J.; Boxall, A.B.A. Effects of Soil Properties on the Uptake of Pharmaceuticals into Earthworms. *Env. Pollut.* **2016**, *213*, 922–931. <https://doi.org/10.1016/j.envpol.2016.03.044>.
17. Carter, L.J.; Garman, C.D.; Ryan, J.; et al. Fate and Uptake of Pharmaceuticals in Soil-Earthworm Systems. *Env. Sci. Technol.* **2014**, *48*, 5955–5963. <https://doi.org/10.1021/es500567w>.
18. Selby, K.G.; Korte, C.E.; Phan, L.H.; et al. Method Optimization for Benchtop Mass Spectrometry Imaging of Lipids in *Eisenia Hortensis*. *Front. Environ. Chem.* **2024**, *5*, 1334207. <https://doi.org/10.3389/fenvc.2024.1334207>.

19. Wu, X.; Conkle, J.L.; Ernst, F.; et al. Treated Wastewater Irrigation: Uptake of Pharmaceutical and Personal Care Products by Common Vegetables under Field Conditions. *Environ. Sci. Technol.* **2014**, *48*, 11286–11293. <https://doi.org/10.1021/es502868k>.
20. Dovletyarova, E.A.; Tapia-Pizarro, F.; Ermakov, A.I.; et al. Copper Toxicity Thresholds for Earthworm *Dendrobaena Veneta*: Insights from a Site with Unique Monometallic Soil Contamination. *Environ. Toxicol. Chem.* **2025**, *44*, vgaf155. <https://doi.org/10.1093/etojnl/vgaf155>.
21. OuYang, C.; Chen, B.; Li, L. High Throughput In Situ DDA Analysis of Neuropeptides by Coupling Novel Multiplex Mass Spectrometric Imaging (MSI) with Gas-Phase Fractionation. *J. Am. Soc. Mass Spectrom.* **2015**, *26*, 1992–2001. <https://doi.org/10.1007/s13361-015-1265-0>.
22. Davis, R.B.; Hoang, J.A.; Rizzo, S.M.; et al. Quantitation and Localization of Beta-Blockers and SSRIs Accumulation in Fathead Minnows by Complementary Mass Spectrometry Analyses. *Sci. Total Environ.* **2020**, *741*, 140331. <https://doi.org/10.1016/j.scitotenv.2020.140331>.
23. Selby, K.G.; Hubecky, E.M.; Zerda-Pinto, V.; et al. Mass Spectrometry Imaging for Environmental Sciences: A Review of Current and Future Applications. *Trends Environ. Anal. Chem.* **2024**, *42*, e00232. <https://doi.org/10.1016/j.teac.2024.e00232>.
24. Körber, A.; Anthony, I.G.M.; Heeren, R.M.A. Mass Spectrometry Imaging. *Anal. Chem.* **2025**, *97*, 15517–15549. <https://doi.org/10.1021/acs.analchem.4c05249>.
25. Germershausen, J.I.; Hunt, V.M.; Bostedor, R.G.; et al. Tissue Selectivity of the Cholesterol-Lowering Agents Lovastatin, Simvastatin and Pravastatin in Rats In Vivo. *Biochem. Biophys. Res. Commun.* **1989**, *158*, 667–675. [https://doi.org/10.1016/0006-291X\(89\)92773-3](https://doi.org/10.1016/0006-291X(89)92773-3).
26. van Agthoven, M.A.; Barrow, M.P.; Chiron, L.; et al. Differentiating Fragmentation Pathways of Cholesterol by Two-Dimensional Fourier Transform Ion Cyclotron Resonance Mass Spectrometry. *J. Am. Soc. Mass. Spectrom.* **2015**, *26*, 2105–2114. <https://doi.org/10.1007/s13361-015-1226-7>.
27. Goncalves, I.L.; Tal, S.; Barki-Harrington, L.; et al. Conserved Statin-Mediated Activation of the P38-MAPK Pathway Protects *Caenorhabditis Elegans* from the Cholesterol-Independent Effects of Statins. *Mol. Metab.* **2020**, *39*, 101003. <https://doi.org/10.1016/j.molmet.2020.101003>.